



OPEN ACCESS

EDITED BY

Svjetlana Miocinovic,
Emory University, United States

REVIEWED BY

Andrea Protzner,
University of Calgary, Canada
Darren Clark,
University of Calgary, Canada

*CORRESPONDENCE

David A. Borton
✉ david_borton@brown.edu

†These authors share last authorship

RECEIVED 08 September 2023

ACCEPTED 26 December 2023

PUBLISHED 12 January 2024

CITATION

Allawala A, Bijanki KR, Oswald D, Mathura RK, Adkinson J, Pirtle V, Shofty B, Robinson M, Harrison MT, Mathew SJ, Goodman WK, Pouratian N, Sheth SA and Borton DA (2024) Prefrontal network engagement by deep brain stimulation in limbic hubs. *Front. Hum. Neurosci.* 17:1291315. doi: 10.3389/fnhum.2023.1291315

COPYRIGHT

© 2024 Allawala, Bijanki, Oswald, Mathura, Adkinson, Pirtle, Shofty, Robinson, Harrison, Mathew, Goodman, Pouratian, Sheth and Borton. This is an open-access article distributed under the terms of the [Creative Commons Attribution License \(CC BY\)](https://creativecommons.org/licenses/by/4.0/). The use, distribution or reproduction in other forums is permitted, provided the original author(s) and the copyright owner(s) are credited and that the original publication in this journal is cited, in accordance with accepted academic practice. No use, distribution or reproduction is permitted which does not comply with these terms.

Prefrontal network engagement by deep brain stimulation in limbic hubs

Anusha Allawala^{1,2}, Kelly R. Bijanki³, Denise Oswald⁴, Raissa K. Mathura³, Joshua Adkinson³, Victoria Pirtle³, Ben Shofty⁵, Meghan Robinson³, Matthew T. Harrison⁶, Sanjay J. Mathew⁷, Wayne K. Goodman⁷, Nader Pouratian⁸, Sameer A. Sheth^{3†} and David A. Borton^{1,9*†}

¹School of Engineering, Brown University, Providence, RI, United States, ²Department of Neurological Surgery, University of California, San Francisco, San Francisco, CA, United States, ³Department of Neurosurgery, Baylor College of Medicine, Houston, TX, United States, ⁴Department of Neurosurgery, University of Pennsylvania, Philadelphia, PA, United States, ⁵Department of Neurosurgery, University of Utah, Salt Lake City, UT, United States, ⁶Division of Applied Mathematics, Brown University, Providence, RI, United States, ⁷Menninger Department of Psychiatry and Behavioral Sciences, Baylor College of Medicine, Houston, TX, United States, ⁸Department of Neurological Surgery, UT Southwestern Medical Center, Dallas, TX, United States, ⁹Department of Veterans Affairs, Center for Neurorestoration and Neurotechnology, Providence, RI, United States

Prefrontal circuits in the human brain play an important role in cognitive and affective processing. Neuromodulation therapies delivered to certain key hubs within these circuits are being used with increasing frequency to treat a host of neuropsychiatric disorders. However, the detailed neurophysiological effects of stimulation to these hubs are largely unknown. Here, we performed intracranial recordings across prefrontal networks while delivering electrical stimulation to two well-established white matter hubs involved in cognitive regulation and depression: the subcallosal cingulate (SCC) and ventral capsule/ventral striatum (VC/VS). We demonstrate a shared frontotemporal circuit consisting of the ventromedial prefrontal cortex, amygdala, and lateral orbitofrontal cortex where gamma oscillations are differentially modulated by stimulation target. Additionally, we found participant-specific responses to stimulation in the dorsal anterior cingulate cortex and demonstrate the capacity for further tuning of neural activity using current-steered stimulation. Our findings indicate a potential neurophysiological mechanism for the dissociable therapeutic effects seen across the SCC and VC/VS targets for psychiatric neuromodulation and our results lay the groundwork for personalized, network-guided neurostimulation therapy.

KEYWORDS

deep brain stimulation (DBS), major depressive disorder (MDD), ventral capsule/ventral striatum, subcallosal cingulate, gamma oscillations, prefrontal networks, stereo-EEG/intracranial recordings

1 Introduction

The ability to regulate complex emotions and make controlled decisions are central to the human experience and critical for successful navigation through challenging life circumstances. Neuroimaging and electrodiagnostic studies have implicated prefrontal networks encompassing the dorsal anterior cingulate cortex (dACC), orbitofrontal cortex (OFC), ventromedial prefrontal cortex (vmPFC) and amygdala in affective and emotional regulation (Delgado et al., 2008; Etkin et al., 2011, 2015; Groenewold et al., 2013; Hiser and Koenigs, 2018), decision making and impulsivity (Elliott et al., 2000; Shenhav et al., 2013; Hiser and Koenigs, 2018), reward evaluation (Bush et al., 2002; Lipsman et al., 2014; Saez et al., 2018; Knudsen and Wallis, 2020), and emotional processing (Pessoa and Adolphs, 2010; Geissberger et al., 2020). Within electrophysiology studies spanning across species, both low and high frequency oscillations across prefrontal, limbic and cingulate structures have emerged as key signals involved in distinct aspects of cognitive, affective and reward processing. Examples of such signals include theta band (4–8 Hz) and gamma band activity (60–140) in the dACC (Rothé et al., 2011; Heilbronner and Hayden, 2016; Widge et al., 2019) for cognitive control processing and adaptation, respectively, alongside gamma activity for conflict processing in the OFC (Tang et al., 2016). Similarly, theta, beta (13–35 Hz) and gamma activity have emerged as critical neural features representing reward valuation, expectation, modulation and processing the OFC (van Wingerden et al., 2010; Sacré et al., 2016; Saez et al., 2018; Knudsen and Wallis, 2020; Amarante and Laubach, 2021). These spectral features are also modulated in the vmPFC and dACC during affective processing (Lipsman et al., 2014; Bijanzadeh et al., 2022). Of note, depending on anatomical structure and their associated role in executive, affective or reward function, some distinct spectral features have shown to be replicable across species and some studies (e.g., midfrontal and cingulate theta oscillations in cognitive control function). Disruption of neural activity in these implicated circuits is thought to lead to psychiatric disorders of mood, anxiety, and impulsivity, among other behavioral manifestations (Price and Drevets, 2010; Groenewold et al., 2013; Cheng et al., 2016; Williams, 2016; Ferri et al., 2017; Damborská et al., 2020; Rolls et al., 2020). Further, causal manipulations of networks underlying regulation of emotional and cognitive processing using electrical stimulation and lesioning have provided further evidence of the close relationship between disrupted neural circuits and behavioral symptoms in psychiatric disorders (Drevets, 2007; Wilson et al., 2014; Heilbronner et al., 2016; Schneider and Koenigs, 2017; Basu et al., 2019; Sawada et al., 2022). Neuromodulatory interventions (Mayberg et al., 2005; Scangos et al., 2021a) are often used to treat such disorders, but little is known about the human *electrophysiology* of these prefrontal regions in psychiatric disorders and how chronic neurostimulation therapies *modify* circuit dynamics underlying psychiatric symptoms. Characterizing the specific spatiotemporal prefrontal network activity implicated in affective and cognitive processing in response to therapeutic stimulation can inform stimulation paradigms on a chronic or adaptive basis and aid the prediction of an individual's response to stimulation.

Two well-characterized affective hubs previously demonstrated to be gateways to parsimoniously engage prefrontal and corticolimbic networks through invasive means (Mayberg et al., 2005; Quraan et al., 2014; Widge et al., 2019; Elias et al., 2022) are the ventral capsule/ventral striatum (VC/VS) and subcallosal cingulate (SCC). The VC/VS and SCC are thought to be hubs (Crowell et al., 2014) at the crossroads of white matter pathways hypothesized to influence executive function (Widge et al., 2019), reward processing (Rogers et al., 2004; Heldmann et al., 2012) and mood processing (Mayberg et al., 2005; Malone et al., 2009) through their connections of varying degrees to prefrontal and limbic structures (spanning the amygdala, PFC and ACC) (Haber, 2012; Heilbronner and Haber, 2014) with partial overlap (Gutman et al., 2009; Riva-Posse et al., 2014; Zhu et al., 2021). Modulation of the two targets have shown promising results in DBS studies showing improvement in symptoms of anxiety (Lipsman et al., 2013), depression (Mayberg et al., 2005; Holtzheimer et al., 2012; Ramasubbu et al., 2013), treatment-refractory anorexia nervosa (Lipsman et al., 2017), addiction (Mantione et al., 2010; Voges et al., 2013; Kuhn et al., 2014) and obsessive compulsive disorder (Smith et al., 2020; van der Vlis et al., 2021). In the clinical treatment of treatment-resistant depression (TRD) with deep brain stimulation (DBS), the VC/VS and SCC targets both showed initially promising open-label studies (Mayberg et al., 2005; Malone et al., 2009). However, these studies were followed up by controlled trials that failed to meet sufficient outcomes measures ultimately needed for regulatory use of DBS for treatment refractory depression (Dougherty et al., 2015; Holtzheimer et al., 2017). Of interest, while both targets can have an antidepressant effect, responses to stimulation across the two targets are phenotypically different, and notable qualitative differences in behavioral responses (“activating” vs. “calming”) (Mayberg et al., 2005; Malone et al., 2009; Choi et al., 2015; Scangos et al., 2021b; Sheth et al., 2021) have been observed. Prefrontal targets appear to be key in driving a response from both DBS targets (Brown et al., 2020; Clark et al., 2020; Liebrand et al., 2020).

The aim of our study was to evaluate the network-level effects of acute stimulation *between* the SCC and VC/VS, two well-established targets used for psychiatric DBS therapy. We took advantage of a unique opportunity afforded through an ongoing clinical trial of DBS for TRD (NCT03437928) where we performed acute stimulation experiments using segmented DBS leads in the SCC and VC/VS with concurrent high-density intracranial recordings providing high spatiotemporal resolution of neural activity in two participants with TRD. We aimed to characterize the *differences* in neural response across prefrontal networks between the two DBS targets within and across patients with TRD. Given the phenotypic differences that are observable following stimulation of the VC/VS and SCC, and established role of low and high oscillations in the vmPFC, OFC, dACC and amygdala in neuropsychiatric disorders (Drevets, 2007; Myers-Schulz and Koenigs, 2012; Ferri et al., 2017; Rao et al., 2018; McTeague et al., 2020), we hypothesized that we would find differentiable neurophysiological responses to acute stimulation between the DBS targets in our aforementioned regions of interest (OFC, vmPFC, dACC, amygdala) that this would be unique to anatomical regions in high frequency activity (defined as 13–100 Hz for this study) or low frequency activity (defined as 1–13 Hz for our study) building on recent work implicating frequency-specific neural oscillations in

mood (Lipsman et al., 2014; Rao et al., 2018; Scangos et al., 2021a; Bijanzadeh et al., 2022). Our results lay the groundwork for a more mechanistic understanding of the effects of DBS across prefrontal circuits in psychiatric disease, and better equip us to implement optimized, network-guided neuromodulation in the future.

2 Materials and methods

2.1 Participant and study overview

Data for this study was collected from two participants (37 year old Latino male and a 57 year old Caucasian female) diagnosed with TRD. The participants were enrolled in an ongoing clinical trial (NCT 03437928) for DBS for TRD. Each participant gave fully informed consent according to study sponsor guidelines, and all procedures were approved by the local institutional review board at Baylor College of Medicine IRB (H-43036) prior to participation. The trial has enrolled more than two participants, but due to the changing nature of the goals of the study, certain aspects of the stimulation experiments have changed across participants. In particular, the stimulation paradigm (described below in section “2.3 Electrode stimulation and recording”) for the first two participants changed such that the analyses described here were not possible in subsequent participants. Rather than combining heterogeneous analyses, we focused on the data from these first two participants with consistent acquired data.

Participants underwent stereotactic implantation of four DBS leads (Boston Scientific Cartesia, Marlborough, MA, USA) and 10 temporary sEEG electrodes (PMT, Chanhassen, MN, USA) based on pre-operative scans including patient-specific tractography. Post-implantation, patients underwent a 10-day intracranial monitoring period for evaluation of brain networks involved in depression. Following the intracranial monitoring period, sEEG electrodes were removed and the four DBS leads were internalized and connected to two implanted pulse generators (IPG) (Boston Scientific Gevia, Marlborough, MA, USA). Additional surgical details have been described previously (Sheth et al., 2021).

2.2 Electrode implantation

Intracranial sEEG electrodes for local field potential (LFP) recordings were implanted bilaterally across several cortical and subcortical targets based on previous work implicating their roles in mood, reward, as well as cognitive and affective processing (Miller, 2000; Etkin et al., 2015; Knudsen and Wallis, 2020; Friedman and Robbins, 2021). Regions sampled included the dorsolateral prefrontal cortex (dlPFC), ventromedial prefrontal cortex (vmPFC), dorsal anterior cingulate cortex (dACC), lateral and medial orbitofrontal cortex (lOFC, mOFC), superior frontal gyrus (SFG), superior and medial temporal gyri (STG, MTG) and the amygdala (Figure 1A). Post-operative CT scans and pre-operative MRI scans were aligned using the Functional Magnetic Resonance Imaging for the Brain Software Library’s (FMRIB’s) Linear Image Registration Tool (FLIRT). Electrode coordinates were manually determined from the co-registered CT in BioImage Suite and placed into native MRI space. The reconstructed cortical

surface, segmented cortical and subcortical structures and electrode coordinates were visualized using the Multi-Modal Visualization Tool (Felsenstein et al., 2019).

Both participants were implanted bilaterally with segmented DBS leads in the VC/VIS and the SCC, capable of current steering. The DBS leads used in our study consist of eight stimulation contacts: solid ring contacts at the deepest and shallow positions, as well as three-way segmented contacts located between the ring contacts. Seven total contact configurations of interest were identified per lead, including three stacked configurations listed as follows: (1) anterior-facing contacts 2 and 5, (2) posterior-left facing contacts 4 and 7 and (3) posterior-right facing contacts 3 and 6. The remaining four configurations tested were ring configurations listed as follows: (1) solid ring contact 1 (2) solid ring contact 8 (3) combination of segmented ring contacts 2, 3, and 4, and (4) combination of segmented ring contacts 5, 6, and 7 (Figure 1B).

2.3 Electrode stimulation and recording

Monopolar cathodic stimulation was delivered through each DBS lead via a Blackrock CereStim R96 (Blackrock Microsystems, Salt Lake City, UT). A stimulation amplitude of 4.8–5 mA was delivered at the solid ring contacts, whereas for stacked or ring configurations this amplitude was split evenly among contacts to enable current steering, never exceeding 5 mA in total or at any time a charge density of 30 $\mu\text{C}/\text{cm}^2$. Stimulation was applied at 130 Hz, with a pulse width of 180 μs and interphase gap of 100 μs . In participant A, we tested the seven identified stimulation combinations (3 stacked configurations, 4 ring configurations) for each DBS lead in the SCC, and five combinations (3 stacked configurations, 2 ring configurations) in each DBS lead in the VC/VIS. In participant B, we tested all seven combinations across each of the four DBS leads. Each trial of stimulation consisted of 15 s of stimulation on followed by 10 s without stimulation (Figure 1C). Trials were repeated 5 times per contact configuration per DBS lead seriatim, resulting in 25–35 trials per DBS lead for participant A and 35 trials per DBS lead for participant B.

2.4 Data acquisition and signal processing

Electrophysiological signals from implanted sEEG electrode contacts were recorded using a 256-channel NeuroPort Acquisition System (Blackrock Microsystems, UT, USA) at a sampling rate of 2 kHz, with a hardware high pass filter applied at 0.3 Hz. Recordings from sEEG contacts were analyzed offline using custom scripts written in MATLAB (Mathworks Inc. Natick, MA, USA) and Python. LFP signals were demeaned, decimated to 1 kHz and bandpass filtered between 1 and 250 Hz. A butterworth notch filter was applied to remove line noise at 60, 120, and 180 Hz, respectively. Recordings were bipolar re-referenced by subtracting the activity of adjacent electrode contact pairs. Any channels with excessive noise or without a clear neural signal were removed from the analysis. To evaluate the response of the sampled networks before and after stimulation, we analyzed the

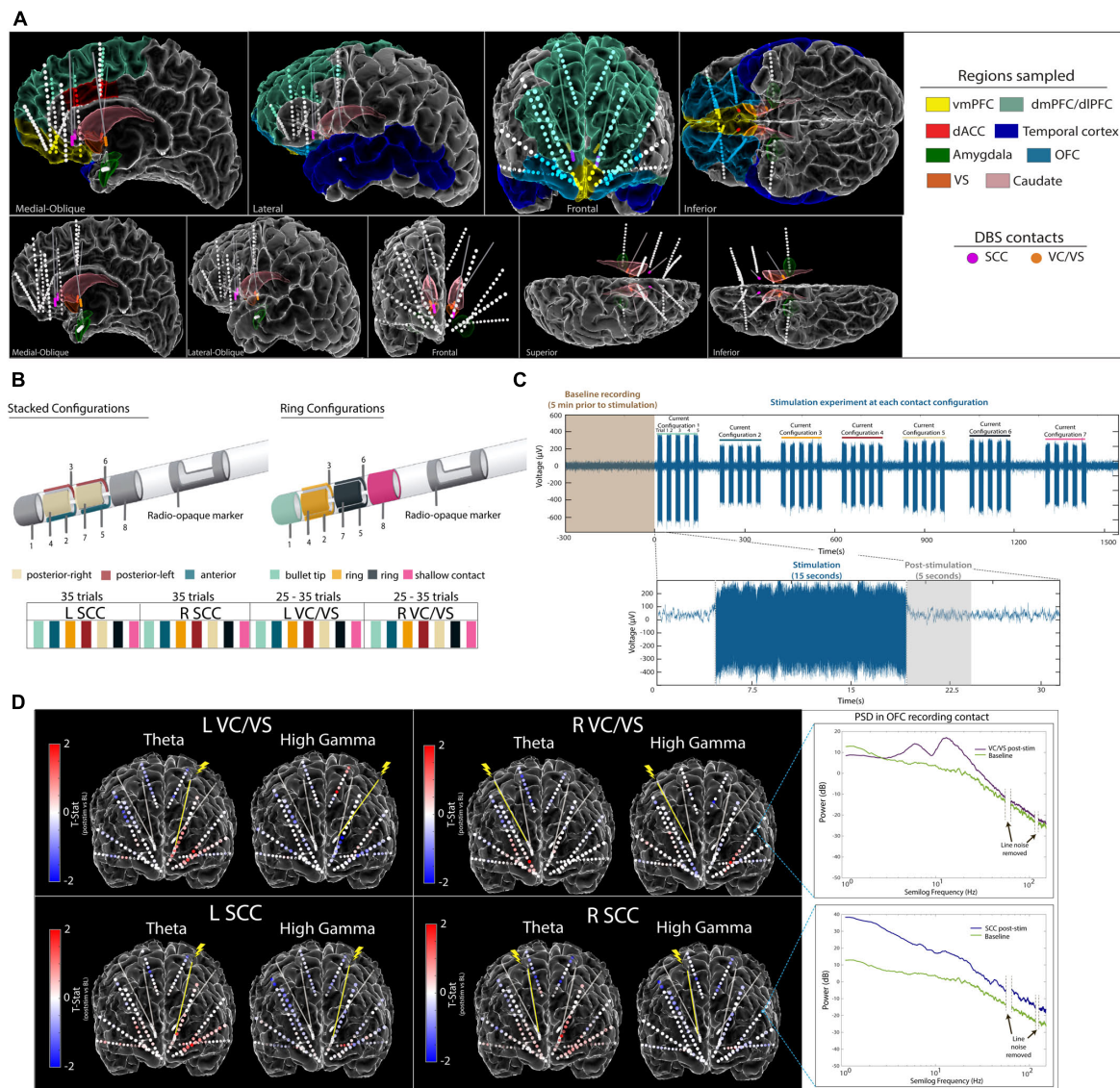


FIGURE 1

Experimental Approach. (A) Anatomical reconstruction showing placement of sEEG electrodes (top panel) and DBS leads (bottom panel). Colors in the legend (right) correspond to the region where electrodes were implanted. The vmPFC, OFC, dACC, and Amygdala were regions of interest for this study. (B) Steerable DBS leads were used to deliver unilateral stimulation in the VC/VS and SCC, respectively. Seven current configurations of interest were identified and tested across participants. (C) Raw voltage signal recorded on an example sEEG contact during stimulation in the left SCC DBS lead. Participants were systematically tested at each current configuration for 15 s, with five trials per current configuration at each respective DBS lead. A 5-s window following stimulation was used for subsequent analyses. (D) Electrode diagram showing the mean power change in theta and high gamma band following stimulation for participant A. Each contact is colored based on the t-statistic value computed between baseline and post-stimulation for each DBS lead (red indicates increase in power following stimulation and blue indicates a decrease in power following stimulation). Inset (right) shows log-transformed power spectra from a recording electrode in the OFC during baseline and post-stimulation. vmPFC, ventromedial prefrontal cortex; IOFC, lateral orbitofrontal cortex; mOFC, medial orbitofrontal cortex; dACC, dorsal anterior cingulate cortex; VC/VS, ventral capsule/ventral striatum; SCC, subcallosal cingulate.

spectral power in the 5 s following stimulation to avoid artifact contamination. We identified a window of 600 ms post-stimulation that was additionally excluded from analysis to avoid residual post-stimulation artifacts in the signal. The multitaper spectral estimation method was used to extract power spectral density (PSD) from the sEEG recording using the *mspectrumc.m* function from the Chronux toolbox (Bokil et al., 2010). Spectral power was then averaged within standard frequency bands (delta = 1–4 Hz, theta = 4–8 Hz, alpha = 8–12 Hz, beta = 12–30 Hz, low-gamma = 30–55 Hz, high-gamma = 65–100 Hz). The spectral power

across the baseline windows and post-stimulation windows across all stimulation experiments were z-scored within participants. Electrode contacts in gray matter located in the regions of interest were identified and pre-processed signals were then grouped (averaged) per region of interest. The location of electrode contacts in gray matter vs. white matter and the labels for anatomical region of interest was verified by visual review of the MRI and CT by an expert rater (BS).

Prior to starting the stimulation experiments, 5 min of baseline recording was collected for each participant (Figure 1C). To

avoid temporal autocorrelation, the autocorrelation was computed for spectral power within each frequency band of interest and region of interest, across time (**Supplementary Figure 2**). The number of lags t where the autocorrelation was at or below 0.1 and all subsequent autocorrelation values were between 0.1 and -0.1 was identified. Lag t was then used to generate surrogate “trials” from the baseline recording, where t seconds was skipped every 5 s. The resulting 5-s trials were used for analysis to compare against the post-stimulation windows during the stimulation experiments (additional details in **Supplementary Figure 2**).

2.5 Statistical analysis

As this study includes two participants, no conclusions about a clinical population with refractory depression can be drawn. The goal with the described analyses is to identify robust, statistically reliable patterns of stimulation-induced network response observed *within* a given participant that cannot be explained by random variation or chance. In order to carefully control for multiple comparisons as our analyses is performed to assess differences across conditions (pre- and post- stimulation, VC/VS vs. SCC stimulation) across ROIs and neural features, we performed the statistical testing procedures described below.

To test the difference between pre- (baseline) and post-stimulation, non-parametric permutation testing was performed on the z-scored data using custom scripts written in MATLAB. Data labels from post-stimulation and baseline windows were randomly shuffled, and then the absolute value of the t-statistic for a two-sample, pooled variance, t -test was computed for each pair of shuffled data. This procedure was repeated 1000 times. We used a single-step maxT procedure to correct for multiple tests (**Westfall and Stanley Young, 1993; Nichols and Holmes, 2002**), namely, each absolute t-statistic was compared to the distribution (over permutations) of the maximal absolute t-statistic across all regions of interest and frequency bands of interest in order to obtain corrected p -values that control the familywise error rate (corrected p -values reported in **Supplementary Tables 1–4** and uncorrected p -values are reported in **Supplementary Tables 7–10**).

To test the difference between PSD changes across the network following unilateral VC/VS stimulation vs. SCC stimulation, non-parametric permutation testing was performed on the z-scored data using custom scripts written in MATLAB. We compared the effect of unilateral VC/VS to unilateral SCC stimulation (i.e., left VC/VS was tested against left SCC stim and right VC/VS stim was tested against right SCC stim). Data labels for unilateral SCC stimulation and unilateral VC/VS stimulation were randomly shuffled, and then the absolute value of the t-statistic for a two-sample, pooled variance, t -test was computed for each pair of shuffled data. This procedure was repeated 1000 times. We used a single-step maxT procedure to correct for multiple tests (**Westfall and Stanley Young, 1993; Nichols and Holmes, 2002**), namely, each absolute t-statistic was compared to the distribution (over permutations) of the maximal absolute t-statistic across all regions of interest and frequency bands of interest in order to obtain corrected p -values that control the familywise error rate (corrected p -values reported in **Supplementary Tables 5, 6** and uncorrected

p -values are reported in **Supplementary Tables 11, 12**). Additional details on statistical testing are described in the **Supplementary material**.

3 Results

The goal of our study was to quantify prefrontal network responses to intracranial stimulation between two DBS targets: the SCC and VC/VS. We first evaluated the effects of stimulation for each DBS target (pre- vs. post-stim, p -values adjusted to compensate for multiple comparisons reported in **Supplementary Methods** and **Supplementary Tables 1–4; Figure 1C**) on high-density stereo-EEG (sEEG recordings) in two participants with TRD (**Figures 1A, B** and **Supplementary Methods**). We then compared neural responses (see **Supplementary Methods**) following stimulation between the two DBS targets (SCC post-stim vs. VC/VS post-stim, adjusted p -values reported in **Supplementary Tables 5, 6**) on high frequency neural activity (beta, low gamma and high gamma band power) and low frequency activity (delta, theta and alpha band power). A representative example of the electrode coverage is shown in **Figure 1D**, illustrating bilateral modulation of low frequency power (e.g., theta) and high frequency power (e.g., high gamma) across recording contacts following unilateral stimulation in participant A. Statistical limitations in our study with $N = 2$ participants preclude any conclusions about a broader clinical population. However, identifying differences across conditions *within* a participant that cannot be estimated by chance entails carefully accounting for the multiple testing problem as we have done in our statistical analyses described in the section “2 Materials and methods.”

Given the previously established roles of the dACC, amygdala, OFC and vmPFC in affective and cognitive regulation in psychiatric disorders, we focused our analyses across these key four anatomical regions within each subject and describe our findings for each key region in detail below.

3.1 vmPFC

We first sought to understand the effect of stimulation on high frequency activity in the vmPFC given its broad involvement in cognitive, affective and emotional processing (**Hiser and Koenigs, 2018**), shown in **Figures 2A–F**. Here, we found consistent differences when evaluating neural responses in high frequency bands between SCC and VC/VS stimulation (**Figures 2C, F**) in both participants. **Specifically, we found that SCC consistently increased gamma power in both participants while VC/VS decreased gamma power.** Within Participant A, left SCC stimulation elicited a significant increase in spectral power in high gamma (pre- vs. post-stim, $adj.p < 0.01$). The response to stimulation was significantly different between both DBS targets in high gamma band ($adj.p < 0.01$) and low gamma band ($adj.p < 0.01$) irrespective of the hemisphere of stimulation. The inverse relationship in which SCC increased high-frequency activity and VC/VS decreased high-frequency activity was also observed in beta band ($adj.p < 0.001$) in participant A. In

Participant B (**Figure 2D**), we observed right VC/VS stimulation significantly decreased low gamma power ($\text{adj.}p < 0.05$) and beta power ($\text{adj.}p < 0.001$) from baseline. In the same participant, neural responses were significantly different between the two DBS targets as observed in low gamma ($\text{adj.}p < 0.05$) and high gamma ($\text{adj.}p < 0.01$; **Figure 2F**).

We next explored if the same opposing response between SCC and VC/VS was observed in low-frequency activity. We did observe a significant difference in delta power between SCC and VC/VS stimulation in both participants (**Figures 2C, F**). While both SCC and VC/VS stimulation significantly increased delta power from baseline ($\text{adj.}p < 0.01$), respectively, we found that VC/VS stimulation drove a larger increase in delta power than SCC stimulation and the responses between the two DBS targets were significantly different ($\text{adj.}p < 0.05$) in participant A. In participant B, it appears that while both SCC and VC/VS stimulation drive a decrease in delta power from baseline (**Figure 2D**), the response between the two targets is still significantly different, where VC/VS drives a smaller decrease than SCC stimulation ($\text{adj.}p < 0.01$; **Figure 2F**).

3.2 Amygdala

The next area of interest for this study was the amygdala (**Figures 3A–F**), given its role in emotional regulation (Pessoa and Adolphs, 2010). In the amygdala, **while both VC/VS and SCC stimulation elicited increases in low and high gamma power, responses in both low and high gamma were still significantly different between the DBS targets in both participants (Figures 3C, F)**. SCC stimulation significantly increased high frequency activity from baseline in both participants (**Figures 3A, D**). In participant A, SCC stimulation drove a significant increase in beta ($\text{adj.}p < 0.001$), low gamma ($\text{adj.}p < 0.001$) and high gamma power ($\text{adj.}p < 0.001$). In participant B, right SCC stimulation significantly increased low gamma ($\text{adj.}p < 0.001$) and high gamma power ($\text{adj.}p < 0.001$) while significantly decreasing beta power ($\text{adj.}p < 0.01$). VC/VS stimulation also significantly increased high gamma power in both participants ($\text{adj.}p < 0.05$; **Figures 3A, D**). In participant A, right VC/VS stimulation also significantly increased low gamma power ($\text{adj.}p < 0.05$) and in participant B, left VC/VS stimulation significantly decreased beta power ($\text{adj.}p < 0.05$). When contrasting neural responses between the two DBS targets (**Figures 3C, F**) we observed that SCC increased low gamma ($\text{adj.}p < 0.05$) and high gamma power ($\text{adj.}p < 0.05$) significantly higher than VC/VS stimulation, and right SCC increased beta power significantly higher than VC/VS stimulation ($\text{adj.}p < 0.01$) in participant A. In participant B, beta power and high gamma power were again significantly higher ($\text{adj.}p < 0.05$) following right SCC stimulation compared to right VC/VS stimulation, and low gamma power was significantly higher ($\text{adj.}p < 0.001$) following SCC stimulation compared to VC/VS stimulation irrespective of the hemisphere of stimulation.

Across low frequency bands, we found responses to SCC and VC/VS stimulation were significantly different in theta band in participant B ($\text{adj.}p < 0.01$; **Figures 3C, F**). Here, SCC drove a decrease in power relative to the VC/VS. However, no consistent modulation of low frequency activity across the two participants was otherwise observed.

3.3 Lateral and medial OFC

The IOFC was a third target of interest because it has been implicated in cognitive and reward processing and recently employed as a target for neuromodulation to improve mood (Rao et al., 2018; Scangos et al., 2021b). Results to stimulation between DBS targets are shown in **Figures 4A–F**. We found neural responses to SCC stimulation were significantly different from VC/VS stimulation in participant A ($\text{adj.}p < 0.05$; **Figure 4C**) and once again followed the same inverse relationship seen in the amygdala, **where SCC drove an increase in power in beta, low gamma, and high gamma bands relative to the VC/VS**. In the same participant, SCC stimulation also significantly increased beta, low gamma and high gamma power from baseline ($\text{adj.}p < 0.01$). In participant B, the significant difference in response between SCC and VC/VS stimulation was observed in high gamma power ($\text{adj.}p < 0.01$; **Figure 4F**) following stimulation in the left hemisphere. Surprisingly, we did not find many differences in neural responses to SCC and VC/VS stimulation across lower frequency bands. Delta band power was significantly modulated, ($\text{adj.}p < 0.01$): right VC/VS stimulation increased delta power and right SCC stimulation decreased delta power. The differential delta band power change was, however, participant specific.

We explored stimulation response in the mOFC separately as the lateral and medial orbitofrontal structures have shown to have distinct roles in cognitive and reward processing (Elliott et al., 2000). In the mOFC (**Figures 4G–L**), we found that differences between responses in high frequency activity following SCC vs. VC/VS stimulation were participant specific in the mOFC (**Figures 4I, L**). For example, the inverse relationship where SCC increases high frequency activity and VC/VS decreases high frequency activity was observed in participant A. Here, right SCC stimulation significantly increased beta power from baseline ($\text{adj.}p < 0.001$; **Figure 4G**), and we observed a significant difference in response to stimulation in beta power between the SCC and the VC/VS ($\text{adj.}p < 0.01$, **Figure 4I**). In participant B, SCC significantly increased high gamma power from baseline ($\text{adj.}p < 0.05$; **Figure 4J**). The inverse relationship between SCC and VC/VS stimulation-induced responses of high frequency activity was observed in low gamma ($\text{adj.}p < 0.05$) and high gamma ($\text{adj.}p < 0.01$), where SCC stimulation increased activity relative to VC/VS stimulation (**Figure 4L**).

When assessing stimulation response in low frequency activity in the mOFC, we found significant differences between responses to VC/VS vs. SCC stimulation seen across both participants in delta band (**Figures 4I, L**). In participant A, left VC/VS stimulation significantly increased power in delta band, and this response was significantly higher than the neural response following SCC stimulation ($\text{adj.}p < 0.05$). In participant B, right VC/VS stimulation significantly increased delta power relative to SCC stimulation ($\text{adj.}p < 0.01$).

3.4 dACC

A key region known to play an important role in cognitive control and emotional processing is the dACC (Shenhav et al., 2013; Etkin et al., 2015). In the dACC (**Figures 5A–F**), when examining high frequency activity, we found that significant

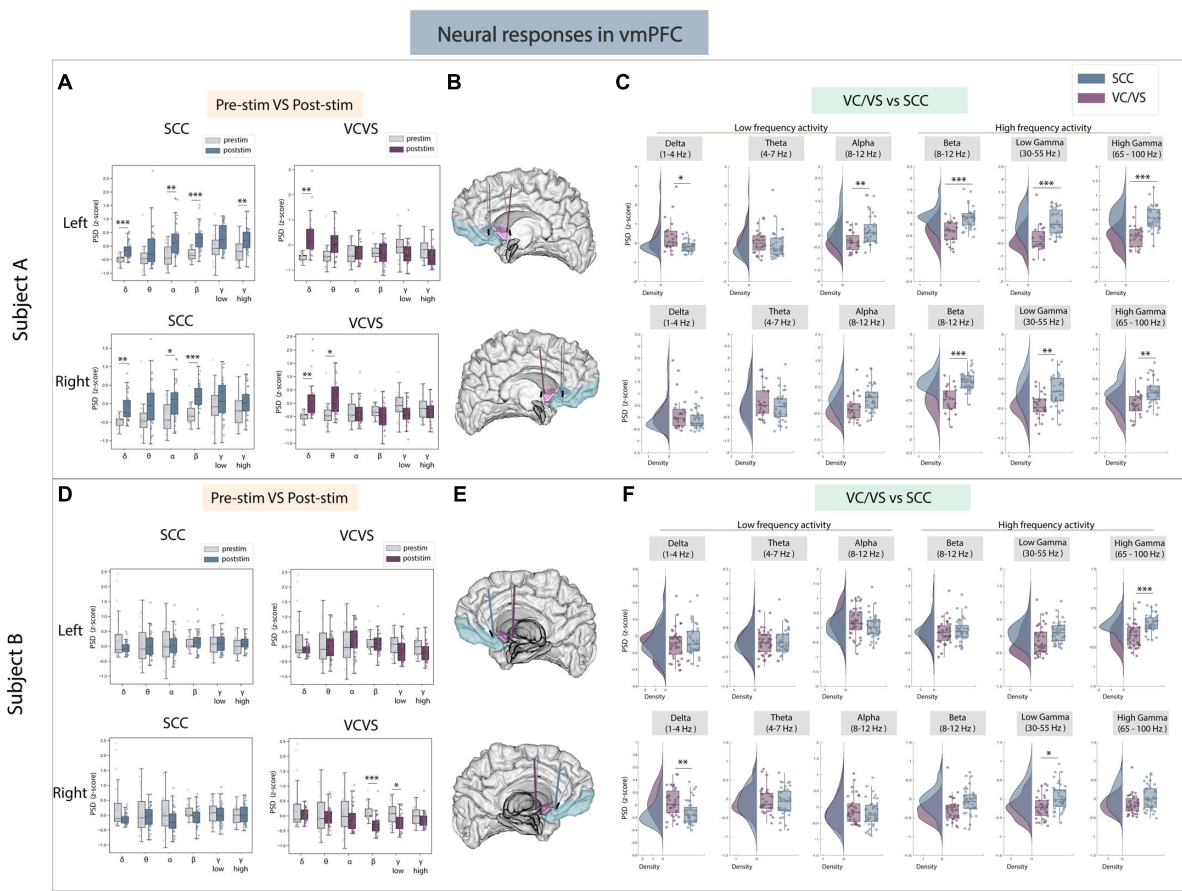


FIGURE 2 Neural responses in the vmPFC following SCC stimulation vs. VC/Vs stimulation. **(A)** Distribution of spectral power across all post-stimulation trials vs. pre-stimulation (baseline) in the vmPFC after z-scoring in six pre-defined frequency bands (delta, theta, alpha, beta, low gamma, and high gamma) following SCC stimulation (left) and VC/Vs stimulation (right) in participant A **(B)** Corresponding anatomical location of the vmPFC highlighted in light blue and corresponding VC/Vs and SCC DBS leads highlighted depending on hemisphere of stimulation. Stimulation in left hemisphere is on top, while stimulation in right hemisphere is shown on the bottom. **(C)** Distribution of spectral power across six pre-defined frequency bands contrasting neural responses following SCC stimulation and VC/Vs stimulation. **(D–F)** Replicate of figures in panels **(A–C)** for participant B. *Indicates significance where $adj.p\text{-value} < 0.05$, corrected; **Indicates significance where $adj.p\text{-value} \leq 0.01$, corrected; ***Indicates significance, where $adj.p\text{-value} \leq 0.001$, corrected.

differences following stimulation between the SCC and VC/Vs were also individual-specific in the dACC but still followed the inverse relationship between the two DBS targets observed in high frequency activity in other ROIs (Figures 5C, F). Right SCC stimulation significantly increased beta power ($adj.p < 0.01$) compared to VC/Vs stimulation in participant A. In participant B, left SCC stimulation significantly increased low gamma power from baseline ($adj.p < 0.01$) while stimulation of either hemisphere in the SCC increased high gamma power ($adj.p < 0.001$; Figure 5D). Left VC/Vs stimulation similarly significantly increased low gamma power ($adj.p < 0.05$) while stimulation of either hemisphere significantly increased high gamma power from baseline ($adj.p < 0.01$; Figure 5D). However, the responses between left SCC and left VC/Vs stimulation were still significantly different in low gamma band ($adj.p < 0.01$; Figure 5F) and SCC stimulation drove a larger increase in low gamma power relative to the VC/Vs.

When examining low frequency activity in response to stimulation in the dACC, we also observed a significant difference between VC/Vs and SCC stimulation in delta power ($adj.p < 0.001$)

in participant B—similar to the pattern observed in other ROIs—where SCC decreased power in a low frequency band (delta) and VC/Vs stimulation increased power. In participant A, right SCC stimulation significantly decreased delta power ($adj.p < 0.05$) but no significant difference was observed between SCC and VC/Vs stimulation in delta power.

4 Discussion

Through a unique intracranial stimulation and recording dataset collected in two participants with TRD, we obtained results with two main conclusions (Figure 6). First, we demonstrate that two canonical targets for psychiatric neuromodulation, the SCC and VC/Vs, elicit network-wide neurophysiological responses in both high and low frequency activity following stimulation. Second, as hypothesized, we show that stimulation in the SCC and VC/Vs drive differentiable neural responses. Specifically, we observed opposite effects on gamma activity in the vmPFC, and

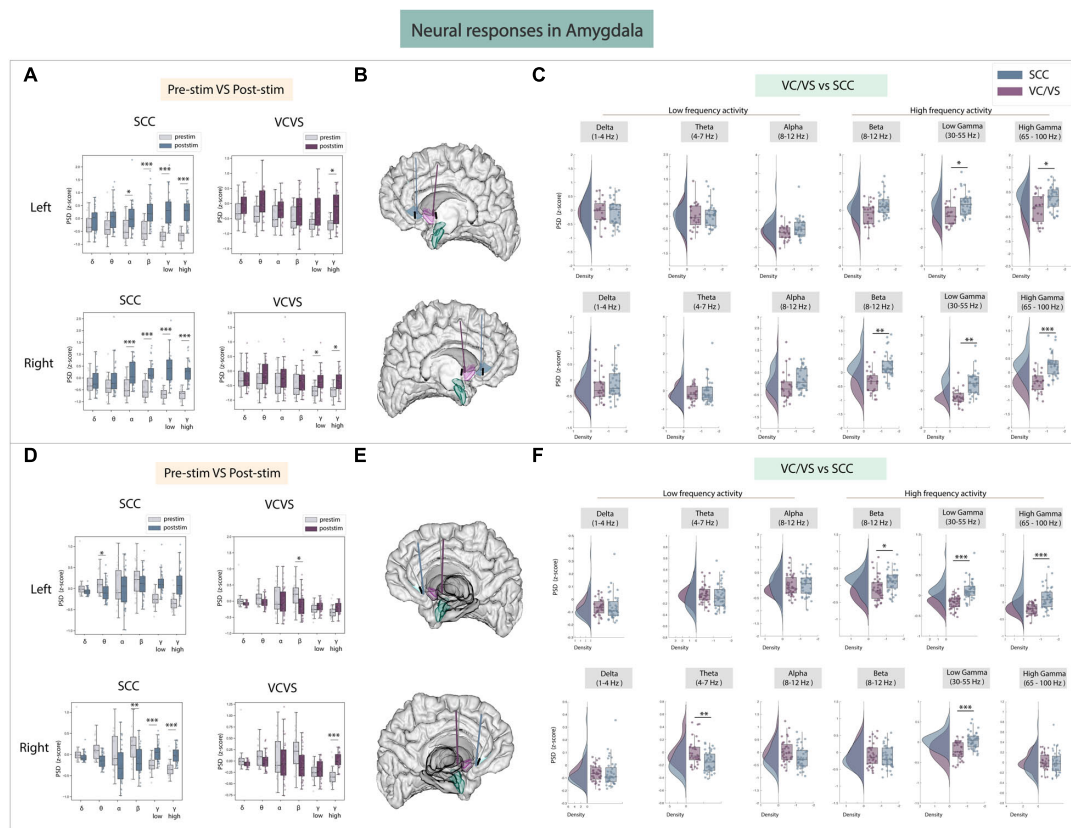


FIGURE 3
 Neural responses in the amygdala following SCC stimulation vs. VC/VS stimulation. **(A)** Distribution of spectral power across all post-stimulation trials vs. pre-stimulation (baseline) in the amygdala after z-scoring in six pre-defined frequency bands (delta, theta, alpha, beta, low gamma, and high gamma) following SCC stimulation (left) and VC/VS stimulation (right) in participant A **(B)** Corresponding anatomical location of the amygdala highlighted in green and corresponding VC/VS and SCC DBS leads highlighted depending on hemisphere of stimulation. Stimulation in left hemisphere is on top, while stimulation in right hemisphere is shown on the bottom. **(C)** Distribution of spectral power across six pre-defined frequency bands contrasting neural responses following SCC stimulation and VC/VS stimulation. **(D–F)** Replicate of figures in panels **(A–C)** for participant B. *Indicates significance where adj.p-value < 0.05, corrected; **Indicates significance where adj.p-value ≤ 0.01, corrected; ***Indicates significance, where adj.p-value ≤ 0.001, corrected.

differing degrees of modulation on gamma activity in the IOFC and amygdala, where SCC stimulation consistently drives a greater increase in gamma oscillations relative to the VC/VS.

Previous tractography work demonstrates that projections from the SCC and VC/VS overlap in the amygdala and medial PFC, but the anatomical trajectory and pattern of connectivity of these projections are distinct (Gutman et al., 2009; Zhu et al., 2021), including the sub-regions that receive projections from the SCC and VC/VS, respectively (Zhu et al., 2021). The difference in connectivity patterns may partially account for the distinct patterns of gamma activity in the vmPFC and amygdala between the two stimulation targets. The modulation of gamma activity seen in the amygdala is additionally supported by a recent study implementing amygdala gamma power as a biomarker for closed-loop VC/VS DBS in a case study for TRD (Scangos et al., 2021a). Interestingly, our results also show modulation of gamma activity in the amygdala following stimulation in both targets, but to differing degrees.

Previous studies have also demonstrated anatomical connectivity between the SCC and the OFC, and the VC/VS and the OFC (Johansen-Berg et al., 2008; Haber, 2016), and initial

results from our group have shown differing effective connectivity between the SCC and VC/VS to the IOFC, respectively, in TRD participants (Adkinson et al., 2022), leading us to expect differences in neural responses between VC/VS and SCC stimulation. While we observed differing degrees of gamma power modulation in the IOFC depending on the DBS target stimulation in both participants, we did not always observe an overlap in neural responses to stimulation between IOFC and mOFC which might be explained in part by previous work indicating the distinct roles of the lateral vs. medial OFC (Cheng et al., 2016; Rao et al., 2018).

While both VC/VS and SCC stimulation can ameliorate depressive symptoms, they have been described to modulate different dimensions of affective processing and mood: VC/VS stimulation has been reported to increase motivation and energy (Malone et al., 2009; Gibson et al., 2017), while SCC stimulation has reportedly increased calmness, alertness and exteroceptive awareness (Choi et al., 2015; Riva-Posse et al., 2019). It is possible that the dissociable increase/decrease in gamma activity in the vmPFC and the differing degree of gamma modulation in the amygdala and IOFC may be underlying the differences in SCC vs. VC/VS stimulation described in acute behavioral reports seen

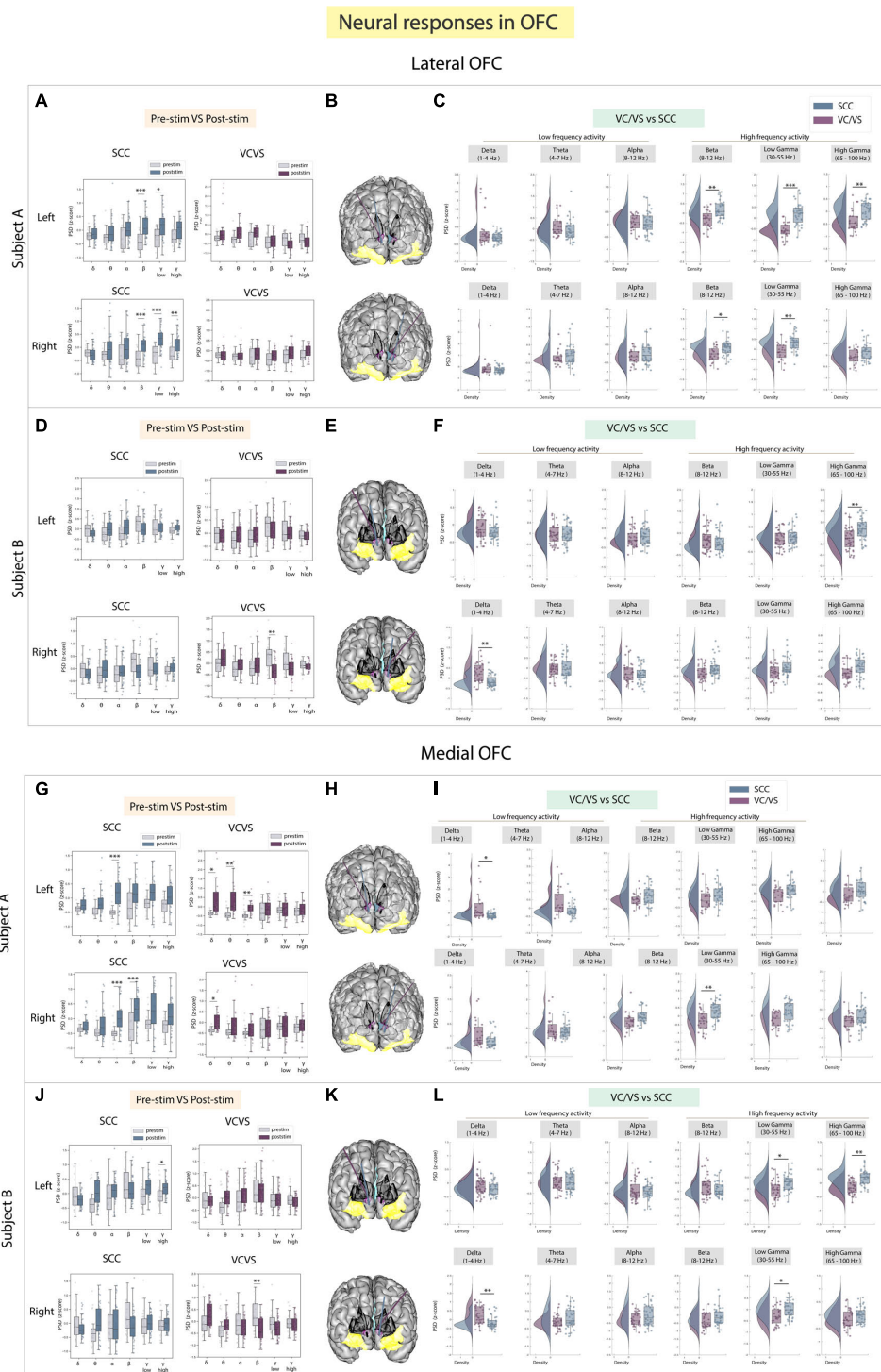


FIGURE 4

Neural responses in the OFC following SCC stimulation vs. VC/Vs stimulation. (A) Distribution of spectral power across all post-stimulation trials vs. pre-stimulation (baseline) in the lOFC after z-scoring in six pre-defined frequency bands (delta, theta, alpha, beta, low gamma, and high gamma) following SCC stimulation (left) and VC/Vs stimulation (right) in participant A (B) Corresponding anatomical location of OFC highlighted in yellow and corresponding VC/Vs and SCC DBS leads highlighted depending on hemisphere of stimulation. Stimulation in left hemisphere is on top, while stimulation in right hemisphere is shown on the bottom. (C) Distribution of spectral power across six pre-defined frequency bands contrasting neural responses following SCC stimulation and VC/Vs stimulation. (D–F) Replicate of figures in panels (A–C) for participant B. (G) Distribution of spectral power across all post-stimulation trials vs. pre-stimulation (baseline) in the mOFC after z-scoring in six pre-defined frequency bands following SCC stimulation (left) and VC/Vs stimulation (right) in participant A. (H) Corresponding anatomical location of OFC highlighted in yellow and corresponding VC/Vs and SCC DBS leads highlighted depending on hemisphere of stimulation. Stimulation in left hemisphere is on top, while stimulation in right hemisphere is shown on the bottom. (I) Distribution of spectral power across six pre-defined frequency bands contrasting neural responses following SCC stimulation and VC/Vs stimulation. (J–L) Replicate of figures in panels (G–I) for participant B. *Indicates significance where $adj.p\text{-value} < 0.05$, corrected; **Indicates significance where $adj.p\text{-value} \leq 0.01$, corrected; ***Indicates significance, where $adj.p\text{-value} \leq 0.001$, corrected.

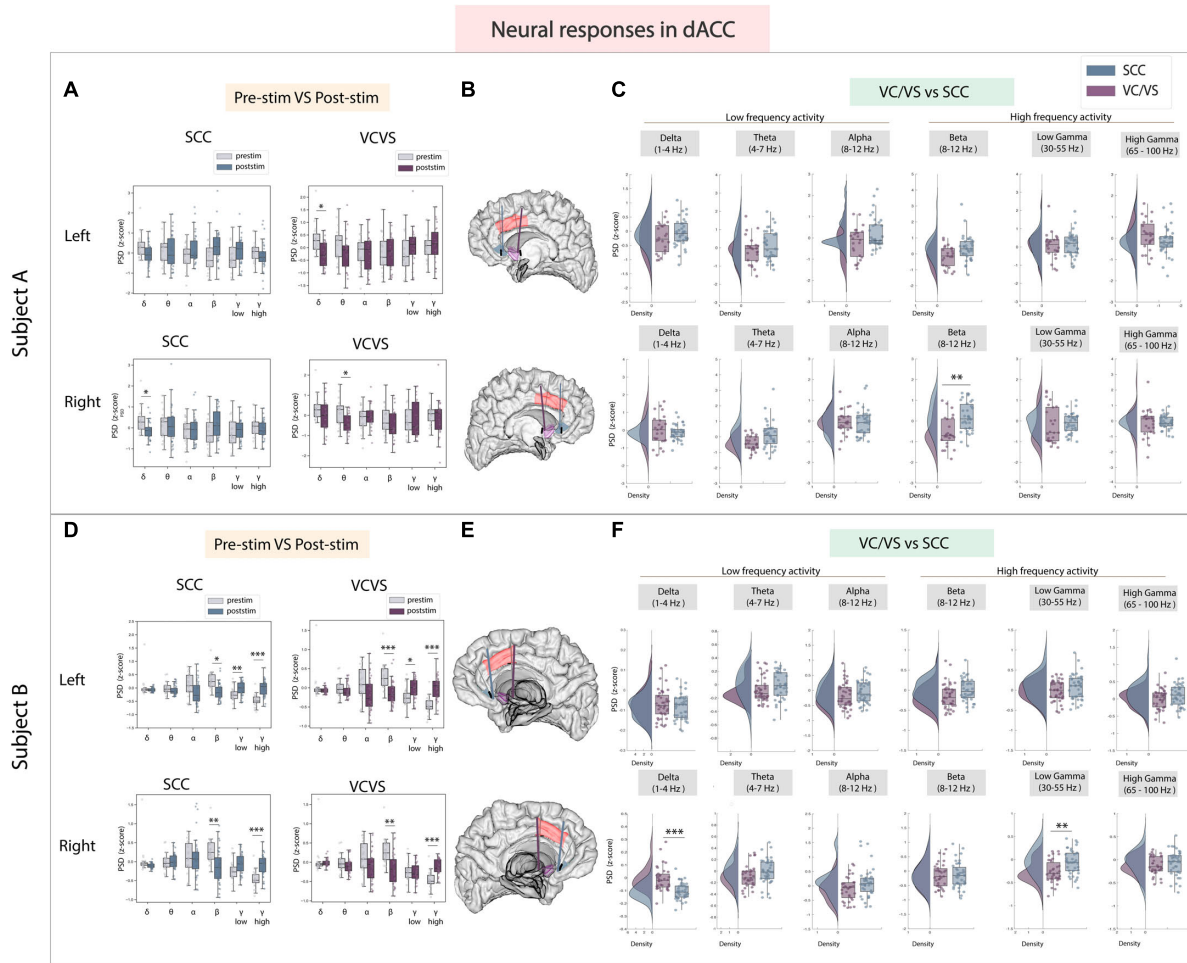


FIGURE 5
 Neural responses in the dACC following SCC stimulation vs. VC/Vs stimulation. **(A)** Distribution of spectral power across all post-stimulation trials vs. pre-stimulation (baseline) in the dACC after z-scoring in six pre-defined frequency bands (delta, theta, alpha, beta, low gamma, and high gamma) following SCC stimulation (left) and VC/Vs stimulation (right) in participant A **(B)** Corresponding anatomical location of dACC highlighted in red and corresponding VC/Vs and SCC DBS leads highlighted depending on hemisphere of stimulation. Stimulation in left hemisphere is on top, while stimulation in right hemisphere is shown on the bottom. **(C)** Distribution of spectral power across six pre-defined frequency bands comparing neural responses between SCC stimulation and VC/Vs stimulation. **(D–F)** Replicate of figures in panels **(A–C)** for participant B. *Indicates significance where $adj.p\text{-value} < 0.05$, corrected; **Indicates significance where $adj.p\text{-value} \leq 0.01$, corrected; ***Indicates significance, where $adj.p\text{-value} \leq 0.001$, corrected.

elsewhere and further work will elucidate our understanding of this phenomenon.

In the dACC, we expected consistent differences in gamma power modulation following SCC and VC/Vs stimulation, given recent work implicating dACC gamma power in positive affective behaviors (Bijanazadeh et al., 2022) and differential connectivity of the dACC to the VC/Vs (Haber, 2016; Baldermann et al., 2021) and SCC (Johansen-Berg et al., 2008). However, differences in gamma responses between SCC and VC/Vs stimulation were participant-specific. Additionally, within a given DBS lead, we observed participant-specific responses between post-stim and pre-stim in the dACC, as well as all other ROIs. The observed participant-specific stimulation responses both between and within the VC/Vs and SCC suggest that increasing efforts to personalize therapy may rely on these within-participant electrophysiological signatures across networks to deliver optimized stimulation. Efforts utilizing participant-specific biomarkers for psychiatric

DBS have been recently successfully demonstrated (Scangos et al., 2021a), alongside network-guided neuromodulation for psychiatric disorders (Cole et al., 2022).

Future efforts incorporating behavioral measures corresponding to functional domains within mental illness, alongside electrophysiological measurements to build brain-behavior relationships with stimulation will help identify generalizable principles that can be potentially extended to sub-domains of MDD in the broader population (Allawala et al., 2021). **Even in the absence of behavioral measurements, characterization of stimulation-induced neural response during resting state, especially between DBS targets, enables tailoring of therapy (i.e., selecting an optimal DBS target and stimulation paradigm) for disorders such as depression, based on a patient’s neural response to stimulation, putative neural biomarker of mood, or another functional domain.** Our study methods currently largely operate as a research

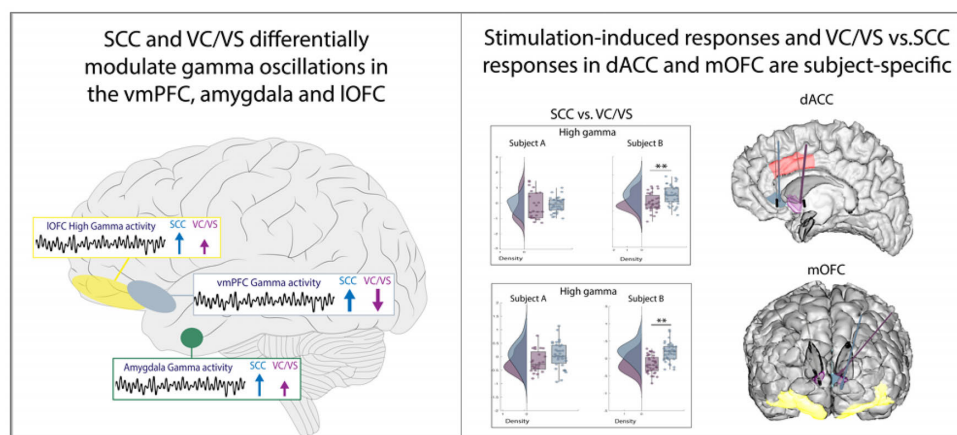


FIGURE 6
Summary of results.

tool, and while subject-specific differences are observable, it is surmised that a greater level of consistency is achievable across a larger cohort of participants as we build on a higher sample size to quantify and model network responses to stimulation, and improve our understanding of biomarkers of symptoms in TRD. For example, as more established neural biomarkers of symptom severity (Xiao et al., 2023) or dysfunctional affective or cognitive processing in patients with TRD are uncovered, some degree of personalization and optimization would be feasible with stimulation across the VC/VS and SCC DBS targets. Indeed, efforts utilizing biomarkers to understand optimal intervention have been recently successfully demonstrated (Alagapan et al., 2023), and network-guided neuromodulation to treat psychiatric disorders has gained traction in recent years. An example of the latter is intermittent theta-burst TMS to treat depression, which currently utilizes resting state functional connectivity between the neuromodulation target of interest for TMS (dlPFC) and the SCC (an extant DBS target) to determine the sub-region for stimulation targeting (Cole et al., 2022), and to predict treatment response outcomes with TMS in the field of non-invasive neuromodulation.

Current-steered DBS provides an added parameter for differentially modulating implicated networks and neural biomarkers. A finer grained approach to precisely target anatomical regions implicated in psychopathology of depression for a desired behavioral responses is needed (Figgie et al., 2022), and the degree of stimulation-induced neural response may plausibly determine a patient's therapeutic response. Future work with a larger number of stimulation trials and participants is needed to understand the extent of the effect that directionality may have on connectivity across prefrontal and limbic networks.

Primary limitations of this study include the small sample size ($N = 2$), and lack of randomization of stimulation conditions within or across the two DBS targets. While a rigorous pipeline for optimal surgical targeting was implemented (Sheth et al., 2021), one possible reason for inconsistent results within and across participants is that small variations in targeting may result in modifications in the electrophysiological effects observed. As we were concerned about insufficient time for stimulation washout between trials and stimulation parameters,

the baseline window used for analysis was a 5-min recording collected prior to stimulation experiments. To address possible temporal autocorrelation in the baseline recording, we performed a correction procedure (Supplementary Figure 2). However, delta power in vmPFC and IOFC in Participant B had a larger amount of autocorrelation during the baseline recording that could not be fully corrected with our approach, thus, results for those specific neural features must be viewed provisionally.

Data availability statement

The raw data supporting the conclusions of this article will be made available by the authors, without undue reservation.

Ethics statement

The studies involving humans were approved by the Baylor College of Medicine Institutional Review Board. The studies were conducted in accordance with the local legislation and institutional requirements. The participants provided their written informed consent to participate in this study.

Author contributions

AA: Conceptualization, Data curation, Formal analysis, Funding acquisition, Investigation, Methodology, Project administration, Visualization, Writing – original draft, Writing – review and editing, Software, Validation. KB: Data curation, Supervision, Writing – review and editing. DO: Resources, Writing – review and editing, Data curation, Investigation, Software. RM: Visualization, Writing – review and editing, Data curation. JA: Data curation, Writing – review and editing. VP: Writing – review and editing, Data curation. BS: Writing – review and editing, Data curation, Resources. MR: Data curation, Writing – review and editing, Software. SM: Writing – review

and editing, Supervision. MH: Writing – review and editing, Supervision, Formal analysis, Methodology, Validation. WG: Writing – review and editing, Supervision, Funding acquisition. NP: Investigation, Resources, Writing – review and editing, Writing – original draft, Funding acquisition, Methodology, Project administration, Supervision. SS: Data curation, Resources, Writing – review and editing, Conceptualization, Funding acquisition, Investigation, Supervision, Visualization, Writing – original draft, Methodology, Project administration. DB: Funding acquisition, Methodology, Supervision, Visualization, Writing – original draft, Writing – review and editing, Investigation.

Funding

The author(s) declare financial support was received for the research, authorship, and/or publication of this article. This study was supported by the National Science Foundation Graduate Research Fellowship (AA), National Institutes of Health grant no. F99 NS124181 (AA), UH3 NS103549 (SS, DB, AA, KB, DO, RM, JA, VP, SM, WG, and NP), grant no. S10 OD025181 (DB), grant no. K01 MH116364 (KB), grant no. NIH R01 MH127006 (KB), grant no. R01 274MH114854 (WG), and the McNair Foundation (SS).

Acknowledgments

We thank our study participants for their dedication and commitment to this study.

Conflict of interest

SS has consulting agreements with Boston Scientific, Neupace, Abbott, and Zimmer Biomet, Varian Medical and Sensoria Therapeutics and is a co-founder for Motif Neurotech. NP was a consultant for Second Sight Medical Products, Abbott Laboratories, Boston Scientific, and Sensoria Therapeutics. WG

References

- Adkinson, J. A., Tsolaki, E., Sheth, S. A., Metzger, B. A., Robinson, M. E., Oswald, D., et al. (2022). Imaging versus electrographic connectivity in human mood-related fronto-temporal networks. *Brain Stimul.* 15, 554–565. doi: 10.1016/j.brs.2022.03.002
- Alagapan, S., Choi, K. S., Heisig, S., Riva-Posse, P., Crowell, A., Tiruvadi, V., et al. (2023). Cingulate dynamics track depression recovery with deep brain stimulation. *Nature* 622, 130–138. doi: 10.1038/s41586-023-06541-3
- Allawala, A., Bijanki, K. R., Goodman, W., Cohn, J. F., Viswanathan, A., Yoshor, D., et al. (2021). A novel framework for network-targeted neuropsychiatric deep brain stimulation. *Neurosurgery* 89, E116–E121. doi: 10.1093/neuros/nyab112
- Amarante, L. M., and Laubach, M. (2021). Coherent theta activity in the medial and orbital frontal cortices encodes reward value. *Elife* 10:e63372. doi: 10.7554/eLife.63372
- Baldermann, J. C., Schüller, T., Kohl, S., Voon, V., Li, N., Hollunder, B., et al. (2021). Connectomic deep brain stimulation for obsessive-compulsive disorder. *Biol. Psychiatry* 90, 678–688. doi: 10.1016/j.biopsych.2021.07.010
- Basu, I., Robertson, M. M., Crocker, B., Peled, N., Farnes, K., Vallejo-Lopez, D. I., et al. (2019). Consistent linear and non-linear responses to invasive electrical brain stimulation across individuals and primate species with implanted electrodes. *Brain Stimul.* 12, 877–892. doi: 10.1016/j.brs.2019.03.007
- Bijanzadeh, M., Khambhati, A. N., Desai, M., Wallace, D. L., Shafi, A., Dawes, H. E., et al. (2022). Decoding naturalistic affective behaviour from spectro-spatial features in multiday human iEEG. *Nat. Hum. Behav.* 6, 823–836. doi: 10.1038/s41562-022-01310-0
- Bokil, H., Andrews, P., Kulkarni, J. E., Mehta, S., and Mitra, P. P. (2010). Chronux: A platform for analyzing neural signals. *J. Neurosci. Methods* 192, 146–151. doi: 10.1016/j.jneumeth.2010.06.020
- Brown, E. C., Clark, D. L., Forkert, N. D., Molnar, C. P., Kiss, Z. H. T., and Ramasubbu, R. (2020). Metabolic activity in subcallosal cingulate predicts response to deep brain stimulation for depression. *Neuropsychopharmacology* 45, 1681–1688. doi: 10.1038/s41386-020-0745-5
- Bush, G., Vogt, B. A., Holmes, J., Dale, A. M., Greve, D., Jenike, M. A., et al. (2002). Dorsal anterior cingulate cortex: A role in reward-based decision making. *Proc. Natl. Acad. Sci. U.S.A.* 99, 523–528. doi: 10.1073/pnas.012470999

has received donated devices from Medtronic, has consulted for Biohaven Pharmaceuticals and receives royalties from Nvive, LLC. SM was supported through the use of resources and facilities at the Michael E. DeBakey VA Medical Center, Houston, Texas and receives support from The Menninger Clinic. SM has served as a consultant to Allergan, Alkermes, Axsome Therapeutics, BioXcel Therapeutics, Clexio Biosciences, COMPASS Pathways, Eleusis, Engrail Therapeutics, Greenwich Biosciences, Intra-Cellular Therapies, Janssen, Levo Therapeutics, Perception Neurosciences, Praxis Precision Medicines, Neumora, Neurocrine, Relmada Therapeutics, Sage Therapeutics, Seelos Therapeutics, and Sunovion. He has received research support from Biohaven Pharmaceuticals, Boehringer-Ingelheim, Janssen, Merck, Sage Therapeutics, and VistaGen Therapeutics.

The remaining authors declare that the research was conducted in the absence of any commercial or financial relationships that could be construed as a potential conflict of interest.

The author(s) declared that they were an editorial board member of Frontiers, at the time of submission. This had no impact on the peer review process and the final decision.

Publisher's note

All claims expressed in this article are solely those of the authors and do not necessarily represent those of their affiliated organizations, or those of the publisher, the editors and the reviewers. Any product that may be evaluated in this article, or claim that may be made by its manufacturer, is not guaranteed or endorsed by the publisher.

Supplementary material

The Supplementary Material for this article can be found online at: <https://www.frontiersin.org/articles/10.3389/fnhum.2023.1291315/full#supplementary-material>

- Cheng, W., Rolls, E. T., Qiu, J., Liu, W., Tang, Y., Huang, C.-C., et al. (2016). Medial reward and lateral non-reward orbitofrontal cortex circuits change in opposite directions in depression. *Brain* 139, 3296–3309. doi: 10.1093/brain/aww255
- Choi, K. S., Riva-Posse, P., Gross, R. E., and Mayberg, H. S. (2015). Mapping the “Depression Switch” during intraoperative testing of subcallosal cingulate deep brain stimulation. *JAMA Neurol.* 72, 1252–1260. doi: 10.1001/jamaneurol.2015.2564
- Clark, D. L., Johnson, K. A., Butson, C. R., Lebel, C., Gobbi, D., Ramasubbu, R., et al. (2020). Tract-based analysis of target engagement by subcallosal cingulate deep brain stimulation for treatment resistant depression. *Brain Stimul.* 13, 1094–1101. doi: 10.1016/j.brs.2020.03.006
- Cole, E. J., Phillips, A. L., Bentzley, B. S., Stimpson, K. H., Nejad, R., Barmak, F., et al. (2022). Stanford Neuromodulation Therapy (SNT): A double-blind randomized controlled trial. *Am. J. Psychiatry* 179, 132–141. doi: 10.1176/appi.ajp.2021.20101429
- Crowell, A. L., Riva-Posse, P., Garlow, S. J., and Mayberg, H. S. (2014). Toward an understanding of the neural circuitry of major depressive disorder through the clinical response to deep brain stimulation of different anatomical targets. *Curr. Behav. Neurosci. Rep.* 1, 55–63. doi: 10.1007/s40473-014-0008-z
- Damborská, A., Honzirková, E., Barteček, R., Hošínková, J., Fedorová, S., Ondruš, Š., et al. (2020). Altered directed functional connectivity of the right amygdala in depression: High-density EEG study. *Sci. Rep.* 10:4398. doi: 10.1038/s41598-020-61264-z
- Delgado, M. R., Nearing, K. I., Ledoux, J. E., and Phelps, E. A. (2008). Neural circuitry underlying the regulation of conditioned fear and its relation to extinction. *Neuron* 59, 829–838. doi: 10.1016/j.neuron.2008.06.029
- Dougherty, D. D., Rezaei, A. R., Carpenter, L. L., Howland, R. H., Bhati, M. T., O’Reardon, J. P., et al. (2015). A randomized sham-controlled trial of deep brain stimulation of the ventral capsule/ventral striatum for chronic treatment-resistant depression. *Biol. Psychiatry* 78, 240–248. doi: 10.1016/j.biopsych.2014.11.023
- Drevets, W. C. (2007). Orbitofrontal cortex function and structure in depression. *Ann. N.Y.Acad. Sci.* 1121, 499–527. doi: 10.1196/annals.1401.029
- Elias, G. J. B., Germann, J., Boutet, A., Loh, A., Li, B., Pancholi, A., et al. (2022). 3T MRI of rapid brain activity changes driven by subcallosal cingulate deep brain stimulation. *Brain* 145, 2214–2226. doi: 10.1093/brain/awab447
- Elliott, R., Dolan, R. J., and Frith, C. D. (2000). Dissociable functions in the medial and lateral orbitofrontal cortex: Evidence from human neuroimaging studies. *Cereb. Cortex* 10, 308–317. doi: 10.1093/cercor/10.3.308
- Etkin, A., Büchel, C., and Gross, J. J. (2015). The neural bases of emotion regulation. *Nat. Rev. Neurosci.* 16, 693–700. doi: 10.1038/nrn4044
- Etkin, A., Egner, T., and Kalisch, R. (2011). Emotional processing in anterior cingulate and medial prefrontal cortex. *Trends Cogn. Sci.* 15, 85–93. doi: 10.1016/j.tics.2010.11.004
- Felsenstein, O., Peled, N., Hahn, E., Rockhill, A. P., Frank, D., Libster, A. M., et al. (2019). Multi-Modal Neuroimaging Analysis and Visualization Tool (MMVT). *arXiv [Preprint]* doi: 10.48550/arXiv.1912.10079
- Ferri, J., Eisendrath, S. J., Fryer, S. L., Gillung, E., Roach, B. J., and Mathalon, D. H. (2017). Blunted amygdala activity is associated with depression severity in treatment-resistant depression. *Cogn. Affect. Behav. Neurosci.* 17, 1221–1231. doi: 10.3758/s13415-017-0544-6
- Figee, M., Riva-Posse, P., Choi, K. S., Bederson, L., Mayberg, H. S., and Kopell, B. H. (2022). Deep brain stimulation for depression. *Neurotherapeutics* 19:1229–1245. doi: 10.1007/s13311-022-01270-3
- Friedman, N. P., and Robbins, T. W. (2021). The role of prefrontal cortex in cognitive control and executive function. *Neuropsychopharmacology* 47:72–89. doi: 10.1038/s41386-021-01132-0
- Geissberger, N., Tik, M., Sladky, R., Woletz, M., Schuler, A.-L., Willinger, D., et al. (2020). Reproducibility of amygdala activation in facial emotion processing at 7T. *Neuroimage* 211:116585. doi: 10.1016/j.neuroimage.2020.116585
- Gibson, W. S., Cho, S., Abulseoud, O. A., Gorny, K. R., Felmlee, J. P., Welker, K. M., et al. (2017). The impact of mirth-inducing ventral striatal deep brain stimulation on functional and effective connectivity. *Cereb. Cortex* 27, 2183–2194. doi: 10.1093/cercor/bhw074
- Groenewold, N. A., Opmeer, E. M., de Jonge, P., Aleman, A., and Costafreda, S. G. (2013). Emotional valence modulates brain functional abnormalities in depression: Evidence from a meta-analysis of fMRI studies. *Neurosci. Biobehav. Rev.* 37, 152–163. doi: 10.1016/j.neubiorev.2012.11.015
- Gutman, D. A., Holtzheimer, P. E., Behrens, T. E. J., Johansen-Berg, H., and Mayberg, H. S. (2009). A tractography analysis of two deep brain stimulation white matter targets for depression. *Biol. Psychiatry* 65, 276–282. doi: 10.1016/j.biopsych.2008.09.021
- Haber, S. N. (2012). “Neuroanatomy of reward: A view from the ventral striatum,” in *Neurobiology of sensation and reward*, ed. J. A. Gottfried (Boca Raton, FL: CRC Press/Taylor & Francis).
- Haber, S. N. (2016). Corticostriatal circuitry. *Dialogues Clin. Neurosci.* 18, 7–21. doi: 10.31887/DCNS.2016.18.1/shaber
- Heilbronner, S. R., and Haber, S. N. (2014). Frontal cortical and subcortical projections provide a basis for segmenting the cingulum bundle: Implications for neuroimaging and psychiatric disorders. *J. Neurosci.* 34, 10041–10054. doi: 10.1523/JNEUROSCI.5459-13.2014
- Heilbronner, S. R., and Hayden, B. Y. (2016). Dorsal anterior cingulate cortex: A bottom-up view. *Annu. Rev. Neurosci.* 39, 149–170. doi: 10.1146/annurev-neuro-070815-013952
- Heilbronner, S. R., Safadi, Z., and Haber, S. N. (2016). “Neurocircuits commonly involved in psychiatric disorders and their stimulation and lesion therapies,” in *Neuromodulation in Psychiatry*, (Chichester: John Wiley & Sons, Ltd), 27–48. doi: 10.1002/9781118801086.ch3
- Heldmann, M., Berding, G., Voges, J., Bogerts, B., Galazky, I., Müller, U., et al. (2012). Deep brain stimulation of nucleus accumbens region in alcoholism affects reward processing. *PLoS One* 7:e36572. doi: 10.1371/journal.pone.0036572
- Hiser, J., and Koenigs, M. (2018). The multifaceted role of the ventromedial prefrontal cortex in emotion, decision making, social cognition, and psychopathology. *Biol. Psychiatry* 83, 638–647. doi: 10.1016/j.biopsych.2017.10.030
- Holtzheimer, P. E., Husain, M. M., Lisanby, S. H., Taylor, S. F., Whitworth, L. A., McClintock, S., et al. (2017). Subcallosal cingulate deep brain stimulation for treatment-resistant depression: A multisite, randomised, sham-controlled trial. *Lancet Psychiatry* 4, 839–849. doi: 10.1016/S2215-0366(17)30371-1
- Holtzheimer, P. E., Kelley, M. E., Gross, R. E., Filkowski, M. M., Garlow, S. J., Barrocas, A., et al. (2012). Subcallosal cingulate deep brain stimulation for treatment-resistant unipolar and bipolar depression. *Arch. Gen. Psychiatry* 69, 150–158. doi: 10.1001/archgenpsychiatry.2011.1456
- Johansen-Berg, H., Gutman, D. A., Behrens, T. E. J., Matthews, P. M., Rushworth, M. F. S., Katz, E., et al. (2008). Anatomical connectivity of the subgenual cingulate region targeted with deep brain stimulation for treatment-resistant depression. *Cereb. Cortex* 18, 1374–1383. doi: 10.1093/cercor/bhm167
- Knudsen, E. B., and Wallis, J. D. (2020). Closed-loop theta stimulation in the orbitofrontal cortex prevents reward-based learning. *Neuron* 106, 537–547.e4. doi: 10.1016/j.neuron.2020.02.003
- Kuhn, J., Möller, M., Treppmann, J. F., Bartsch, C., Lenartz, D., Gruendler, T. O. J., et al. (2014). Deep brain stimulation of the nucleus accumbens and its usefulness in severe opioid addiction. *Mol. Psychiatry* 19, 145–146. doi: 10.1038/mp.2012.196
- Liebrand, L. C., Natarajan, S. J., Caan, M. W. A., Schuurman, P. R., van den Munckhof, P., de Kwaasteniet, B., et al. (2020). Distance to white matter trajectories is associated with treatment response to internal capsule deep brain stimulation in treatment-refractory depression. *Neuroimage Clin.* 28:102363. doi: 10.1016/j.nicl.2020.102363
- Lipsman, N., Kaping, D., Westendorff, S., Sankar, T., Lozano, A. M., and Womelsdorf, T. (2014). Beta coherence within human ventromedial prefrontal cortex precedes affective value choices. *Neuroimage* 85(Pt. 2), 769–778. doi: 10.1016/j.neuroimage.2013.05.104
- Lipsman, N., Lam, E., Volpini, M., Sutandar, K., Twose, R., Giacobbe, P., et al. (2017). Deep brain stimulation of the subcallosal cingulate for treatment-refractory anorexia nervosa: 1 year follow-up of an open-label trial. *Lancet Psychiatry* 4, 285–294. doi: 10.1016/S2215-0366(17)30076-7
- Lipsman, N., Woodside, D. B., Giacobbe, P., Hamani, C., Carter, J. C., Norwood, S. J., et al. (2013). Subcallosal cingulate deep brain stimulation for treatment-refractory anorexia nervosa: A phase 1 pilot trial. *Lancet* 381, 1361–1370. doi: 10.1016/S0140-6736(12)62188-6
- Malone, D. A. Jr., Dougherty, D. D., Rezaei, A. R., Carpenter, L. L., Friehs, G. M., Eskandar, E. N., et al. (2009). Deep brain stimulation of the ventral capsule/ventral striatum for treatment-resistant depression. *Biol. Psychiatry* 65, 267–275. doi: 10.1016/j.biopsych.2008.08.029
- Mantione, M., van de Brink, W., Schuurman, P. R., and Denys, D. (2010). Smoking cessation and weight loss after chronic deep brain stimulation of the nucleus accumbens: Therapeutic and research implications: Case report. *Neurosurgery* 66, E218; discussion E218. doi: 10.1227/01.NEU.0000360570.40339.64
- Mayberg, H. S., Lozano, A. M., Voon, V., McNeely, H. E., Seminowicz, D., Hamani, C., et al. (2005). Deep brain stimulation for treatment-resistant depression. *Neuron* 45, 651–660. doi: 10.1016/j.neuron.2005.02.014
- McTeague, L. M., Rosenberg, B. M., Lopez, J. W., Carreon, D. M., Huemer, J., Jiang, Y., et al. (2020). Identification of common neural circuit disruptions in emotional processing across psychiatric disorders. *Am. J. Psychiatry* 177, 411–421. doi: 10.1176/appi.ajp.2019.18111271
- Miller, E. K. (2000). The prefrontal cortex and cognitive control. *Nat. Rev. Neurosci.* 1, 59–65. doi: 10.1038/35036228
- Myers-Schulz, B., and Koenigs, M. (2012). Functional anatomy of ventromedial prefrontal cortex: Implications for mood and anxiety disorders. *Mol. Psychiatry* 17, 132–141. doi: 10.1038/mp.2011.88
- Nichols, T. E., and Holmes, A. P. (2002). Nonparametric permutation tests for functional neuroimaging: A primer with examples. *Hum. Brain Mapp.* 15, 1–25. doi: 10.1002/hbm.1058

- Pessoa, L., and Adolphs, R. (2010). Emotion processing and the amygdala: From a "low road" to "many roads" of evaluating biological significance. *Nat. Rev. Neurosci.* 11, 773–783. doi: 10.1038/nrn2920
- Price, J. L., and Drevets, W. C. (2010). Neurocircuitry of mood disorders. *Neuropsychopharmacology* 35, 192–216. doi: 10.1038/npp.2009.104
- Quraan, M. A., Protzner, A. B., Daskalakis, Z. J., Giacobbe, P., Tang, C. W., Kennedy, S. H., et al. (2014). EEG power asymmetry and functional connectivity as a marker of treatment effectiveness in DBS surgery for depression. *Neuropsychopharmacology* 39, 1270–1281. doi: 10.1038/npp.2013.330
- Ramasubbu, R., Anderson, S., Haffenden, A., Chavda, S., and Kiss, Z. H. T. (2013). Double-blind optimization of subcallosal cingulate deep brain stimulation for treatment-resistant depression: A pilot study. *J. Psychiatry Neurosci.* 38, 325–332. doi: 10.1503/jpn.120160
- Rao, V. R., Sellers, K. K., Wallace, D. L., Lee, M. B., Bijanzadeh, M., Sani, O. G., et al. (2018). Direct electrical stimulation of lateral orbitofrontal cortex acutely improves mood in individuals with symptoms of depression. *Curr. Biol.* 28, 3893–3902.e4. doi: 10.1016/j.cub.2018.10.026
- Riva-Posse, P., Choi, K. S., Holtzheimer, P. E., McIntyre, C. C., Gross, R. E., Chaturvedi, A., et al. (2014). Defining critical white matter pathways mediating successful subcallosal cingulate deep brain stimulation for treatment-resistant depression. *Biol. Psychiatry* 76, 963–969. doi: 10.1016/j.biopsych.2014.03.029
- Riva-Posse, P., Inman, C. S., Choi, K. S., Crowell, A. L., Gross, R. E., Hamann, S., et al. (2019). Autonomic arousal elicited by subcallosal cingulate stimulation is explained by white matter connectivity. *Brain Stimul.* 12, 743–751. doi: 10.1016/j.brs.2019.01.015
- Rogers, R. D., Ramnani, N., Mackay, C., Wilson, J. L., Jezzard, P., Carter, C. S., et al. (2004). Distinct portions of anterior cingulate cortex and medial prefrontal cortex are activated by reward processing in separable phases of decision-making cognition. *Biol. Psychiatry* 55, 594–602. doi: 10.1016/j.biopsych.2003.11.012
- Rolls, E. T., Cheng, W., and Feng, J. (2020). The orbitofrontal cortex: Reward, emotion and depression. *Brain Commun.* 2:fcaa196. doi: 10.1093/braincomms/fcaa196
- Rothé, M., Quilodran, R., Sallet, J., and Procyk, E. (2011). Coordination of high gamma activity in anterior cingulate and lateral prefrontal cortical areas during adaptation. *J. Neurosci.* 31, 11110–11117. doi: 10.1523/JNEUROSCI.10116-11.2011
- Sacré, P., Kerr, M. S. D., Kahn, K., Gonzalez-Martinez, J., Bulacio, J., Park, H.-J., et al. (2016). Lucky rhythms in orbitofrontal cortex bias gambling decisions in humans. *Sci. Rep.* 6:36206. doi: 10.1038/srep36206
- Saez, I., Lin, J., Stolk, A., Chang, E., Parvizi, J., Schalk, G., et al. (2018). Encoding of multiple reward-related computations in transient and sustained high-frequency activity in human OFC. *Curr. Biol.* 28, 2889–2899.e3. doi: 10.1016/j.cub.2018.07.045
- Sawada, M., Adolphs, R., Dlouhy, B. J., Jenison, R. L., Rhone, A. E., Kovach, C. K., et al. (2022). Mapping effective connectivity of human amygdala subdivisions with intracranial stimulation. *Nat. Commun.* 13:4909. doi: 10.1038/s41467-022-32644-y
- Scangos, K. W., Khambhati, A. N., Daly, P. M., Makhoul, G. S., Sugrue, L. P., Zamanian, H., et al. (2021a). Closed-loop neuromodulation in an individual with treatment-resistant depression. *Nat. Med.* 7, 1696–1700. doi: 10.1038/s41591-021-01480-w
- Scangos, K. W., Makhoul, G. S., Sugrue, L. P., Chang, E. F., and Krystal, A. D. (2021b). State-dependent responses to intracranial brain stimulation in a patient with depression. *Nat. Med.* 27, 229–231. doi: 10.1038/s41591-020-01175-8
- Schneider, B., and Koenigs, M. (2017). Human lesion studies of ventromedial prefrontal cortex. *Neuropsychologia* 107, 84–93. doi: 10.1016/j.neuropsychologia.2017.09.035
- Shenhav, A., Botvinick, M. M., and Cohen, J. D. (2013). The expected value of control: An integrative theory of anterior cingulate cortex function. *Neuron* 79, 217–240. doi: 10.1016/j.neuron.2013.07.007
- Sheth, S. A., Bijanki, K. R., Metzger, B., Allawala, A., Pirtle, V., Adkinson, J. A., et al. (2021). Deep brain stimulation for depression informed by intracranial recordings. *Biol. Psychiatry* 92, 246–251. doi: 10.1016/j.biopsych.2021.11.007
- Smith, E. E., Schüller, T., Huys, D., Baldermann, J. C., Andrade, P., Allen, J. J., et al. (2020). A brief demonstration of frontostriatal connectivity in OCD patients with intracranial electrodes. *Neuroimage* 220:117138. doi: 10.1016/j.neuroimage.2020.117138
- Tang, H., Yu, H.-Y., Chou, C.-C., Crone, N. E., Madsen, J. R., Anderson, W. S., et al. (2016). Cascade of neural processing orchestrates cognitive control in human frontal cortex. *Elife* 5:e12352. doi: 10.7554/eLife.12352
- van der Vlis, T. A. M. B., Ackermans, L., Mulders, A. E. P., Vrij, C. A., Schruers, K., Temel, Y., et al. (2021). Ventral capsule/ventral striatum stimulation in obsessive-compulsive disorder: Toward a unified connectomic target for deep brain stimulation? *Neuromodulation* 24, 316–323. doi: 10.1111/ner.13339
- van Wingerden, M., Vinck, M., Lankelma, J., and Pennartz, C. M. A. (2010). Theta-band phase locking of orbitofrontal neurons during reward expectancy. *J. Neurosci.* 30, 7078–7087. doi: 10.1523/JNEUROSCI.3860-09.2010
- Voges, J., Müller, U., Bogerts, B., Münte, T., and Heinze, H.-J. (2013). Deep brain stimulation surgery for alcohol addiction. *World Neurosurg.* 80, S28.e21–S28.e31. doi: 10.1016/j.wneu.2012.07.011
- Westfall, P. H., and Stanley Young, S. (1993). *Resampling-based multiple testing: Examples and methods for p-value adjustment*. New York, NY: John Wiley & Sons.
- Widge, A. S., Zorowitz, S., Basu, I., Paulk, A. C., Cash, S. S., Eskandar, E. N., et al. (2019). Deep brain stimulation of the internal capsule enhances human cognitive control and prefrontal cortex function. *Nat. Commun.* 10:1536. doi: 10.1038/s41467-019-09557-4
- Williams, L. M. (2016). Precision psychiatry: A neural circuit taxonomy for depression and anxiety. *Lancet Psychiatry* 3, 472–480. doi: 10.1016/S2215-0366(15)00579-9
- Wilson, R. C., Takahashi, Y. K., Schoenbaum, G., and Niv, Y. (2014). Orbitofrontal cortex as a cognitive map of task space. *Neuron* 81, 267–279. doi: 10.1016/j.neuron.2013.11.005
- Xiao, J., Provenza, N. R., Asfour, J., Myers, J., Mathura, R. K., Metzger, B., et al. (2023). Decoding depression severity from intracranial neural activity. *Biol. Psychiatry* 94, 445–453. doi: 10.1016/j.biopsych.2023.01.020
- Zhu, Z., Hubbard, E., Guo, X., Barbosa, D. A. N., Popal, A. M., Cai, C., et al. (2021). A connectomic analysis of deep brain stimulation for treatment-resistant depression. *Brain Stimul.* 14, 1226–1233. doi: 10.1016/j.brs.2021.08.010